DOI: 10.1534/genetics.104.034967

Mutation of *l7Rn3* Shows That *Odz4* Is Required for Mouse Gastrulation

Amy C. Lossie,[1] Hisashi Nakamura,[1] Sharon E. Thomas[2] and Monica J. Justice[3]

Department of Molecular and Human Genetics, Baylor College of Medicine, Houston, Texas 77030

Manuscript received August 12, 2004
Accepted for publication October 8, 2004

ABSTRACT

A mouse homolog of the Drosophila pair-rule gene *Odd Oz* (*Odz4*) maps to the critical region of the *l7Rn3* locus on mouse chromosome 7. Here we show that *Odz4* is an excellent candidate for this allelic series because (1) it spans the entire critical region, (2) the phenotypes correlate with embryonic expression, (3) the complex genetic inheritance of the alleles is consistent with complex transcriptional regulation, and (4) one allele has a mutation in a conserved amino acid. *Odz4* uses five alternate promoters that encode both secreted and membrane-bound proteins. Intragenic complementation of the *l7Rn3* alleles is consistent with these multiple-protein isoforms. Further, the allelic series shows that *Odz4* is required to establish the anterior-posterior axis of the gastrulating mouse embryo and is necessary later for mesoderm-derived tissues such as somites, heart, and skeleton. Sequencing of RT-PCR products from five of the six alleles reveals a nonconservative amino acid change in the *l7Rn3*^{m4} allele. This amino acid is important evolutionarily, as it is conserved to Drosophila. Together, our data indicate that *Odz4* is mutated in the *l7Rn3* allele series and performs roles in the mouse brain, heart, and embryonic patterning similar to those of its Drosophila counterpart.

THE TENEURIN/ODD OZ (TEN/ODZ) protein family contains many members with orthologs identified in mammals, vertebrates, insects, and nematodes (Minet and Chiquet-Ehrismann 2000). The first two members of this gene family (*Ten*^{a} and *Ten*^{m}) were identified in Drosophila during a search for homologs of *Tenascin*, a component of the extracellular matrix (Baumgartner and Chiquet-Ehrismann 1993; Baumgartner *et al.* 1994). This family of transmembrane protein receptors shares a common N terminus, called the TENEURIN intracellular domain, as well as 5–8 TENASCIN-type EGF-like repeats and >20 tyrosine/aspartic acid (YD) repeats, which are related to the rearrangement hotspot (RHS) domains found in bacteria. Orthologs have been identified in seven different species (Minet and Chiquet-Ehrismann 2000). While only one *Ten/Odz* gene, *R13F6.4*, was identified in *Caenorhabditis elegans*, two homologs have been reported in Drosophila (*Ten*^{a} and *Ten*^{m}) and zebrafish (*Ten*^{m3} and *Ten*^{m4}), three have been located in chicken (*Ten1*, *Ten2*, and *Ten4*), and four genes have been cloned from both mouse (*Odz1-4*) and human (*TEN1-4*). Although only one gene has been identified so far in the rat (*Neurestin* α), it is likely that additional homologs will be annotated in the near future.

The full-length TEN/ODZ proteins range in size from 2515 to 2825 amino acids (Minet and Chiquet-Ehrismann 2000). There is 37–41% identity between the vertebrate orthologs and the Drosophila *Ten*^{m} or *Ten*^{a} proteins, indicating that (1) the Drosophila and vertebrate gene duplications occurred after the species diverged and (2) either of the Drosophila homologs could be orthologous to one of the vertebrate *Ten/Odz* genes. *Ten*^{m}*/Odz* is expressed in seven stripes in the blastoderm stage of early embryonic development, which is consistent with the expression of the fly pair-rule genes. During later development, expression is dynamic, but most prominent in the central nervous system (CNS) and heart (Baumgartner *et al.* 1994; Levine *et al.* 1994). *Ten*^{a} also demonstrates a dynamic pattern of developmental expression and is prominent in the CNS, hindgut, and brain (Fascetti and Baumgartner 2002).

One of the mammalian homologs, *Odz4* (formerly *Doc4*), was induced following endoplasmic reticulum stress response in mouse fibroblasts (Wang *et al.* 1998). In an effort to identify the function of *Odz* in mammals, Oohashi *et al.* (1999) cloned the four mouse homologs, *Odz1–4*. These studies demonstrated that all four genes were highly expressed in brain, suggested that the mammalian genes functioned as type II transmembrane proteins, and indicated that each gene contained at least three alternatively spliced transcripts. During brain development, these four genes exhibit distinct, but overlapping, expression profiles (Zhou *et al.* 2003).

Ethylnitrosourea (ENU) mutagenesis screens in the mouse identify novel mutants that have defects in early embryonic development (Nolan *et al.* 1997; Hardisty

[1]These authors contributed equally to this work.

[2]*Present address:* Department of Biochemistry, Cellular and Molecular Biology, University of Tennessee, Knoxville, TN 37996.

[3]*Corresponding author:* Department of Molecular and Human Genetics, Baylor College of Medicine, S413, Houston, TX 77030.
E-mail: mjustice@bcm.tmc.edu

et al. 1999; Rinchik and Carpenter 1999; Hrabe de Angelis and Flaswinkel 2000; Isaacs *et al.* 2000; Nolan *et al.* 2000; Soewarto *et al.* 2000; Alessandrini *et al.* 2001; Graw *et al.* 2002; Vivian *et al.* 2002; Kile *et al.* 2003). A series of alleles at *l7Rn3* was isolated following ENU mutagenesis of a large deletion complex encompassing the *Tyrosinase* (*Tyr*) locus on mouse chromosome 7 (Rinchik and Carpenter 1999). The *l7Rn3* complementation group is composed of six lethal mutations (*m1–m6*) that demonstrate interesting genetic behaviors, including intragenic complementation and a maternal effect (Rinchik and Carpenter 1999).

Odz4 fulfills all of the candidate gene criteria for *l7Rn3*. *Odz4* spans the entire ~700-kb critical region for *l7Rn3* and encodes an ~12-kb full-length transcript that produces different alternatively spliced isoforms. Here, we reveal that *Odz4* has five putative promoters and 44 exons, which include 9 additional exons not previously annotated. Many of these new exons are contained in tissue-specific or developmentally restricted transcripts. We also demonstrate that the *l7Rn3* mutants display a wide range of phenotypes, each of which is indicative of disruption in mesoderm differentiation. Finally, mutation analysis indicates that the *m4* allele contains a nonconservative missense mutation in an amino acid that is conserved through Drosophila. Taken as a whole, our data indicate that *Odz4* plays a major role in mouse gastrulation.

MATERIALS AND METHODS

Mouse strains and embryo analysis: BALB/cRl-males were treated with ENU to generate the *l7Rn3* complementation group, which is tightly linked with the *Tyrosinase* locus. The recovery, breeding scheme, and initial identification of this mutant allelic series was previously described (Rinchik and Carpenter 1993, 1999). These alleles have been designated *m1* ($l7Rn3^{1777SB}$), *m2* ($l7Rn3^{677SB}$), *m3* ($l7Rn3^{2292SB}$), *m4* ($l7Rn3^{4324SB}$), *m5* ($l7Rn3^{6105SB}$), and *m6* ($l7Rn3^{2521SB}$). We bred the mutations onto the FRCH stock, which is maintained at Baylor College of Medicine. The FRCH animals are dark chinchilla and have curly fur and whiskers. This strain, $Tyr^{c\text{-}ch}$ *fr*/$Tyr^{c\text{-}ch}$ *fr*, carries the *chinchilla* allele of the *Tyrosinase* locus and the spontaneous mutant, *frizzy*, which flank the *l7Rn3* mutations. Heterozygotes, which are light chinchilla and have normal fur, will have a Tyr^{c} *m* +/$Tyr^{c\text{-}ch}$ + *fr* genotype. Homozygous mutants are obtained from intercrossing heterozygotes and have a Tyr^{c} *m* +/Tyr^{c} *m* + genotype. Two deletion stocks, $Tyr^{c\text{-}ch}$/$Tyr^{c\text{-}26DVT}$ and $Tyr^{c\text{-}ch}$/$Tyr^{c\text{-}1FDFoHw}$, can be used to generate hemizygous mutants.

Embryos were obtained from timed matings. The day of the vaginal plug was designated 0.5. Embryos were visually observed and photographed under a dissecting microscope for stage classification.

Genotyping: Embryos and adult tissues were genotyped with *D7Mit352* and/or *D7Al7*. DNA was isolated from adult tissues using proteinase K digestion and phenol/chloroform extraction according to well-established protocols. DNA was obtained from embryos following a modified proteinase K (Life Technologies, Gaithersburg, MD) digestion. Briefly, embryos were incubated in 1× PCR buffer (Life Technologies) supplemented with 0.08 mg/ml proteinase K for 2–3 hr at 55° and then heated to 95° for 10 min to deactivate the proteinase K. Embryos dissected at or before E9.5 were incubated in 25 μl of 1× PCR buffer, while embryos older than E9.5 were digested in a final volume of 100 μl. Genotyping was performed on 10–200 ng of genomic DNA. After an initial denaturing step at 95° for 5 min, *D7Mit352* was amplified with the following cycling parameters: 30 cycles of 94° for 30 sec, 58° for 30 sec followed by 72° for 30 sec, with a final 5-min incubation at 72°. Products were size fractionated on 5% metaphor, 1× TBE or 6% native polyacrylamide, 1× TBE gels. Acrylamide gels were electrophoresed for 18 hr at 35 V. *D7Al7* was amplified according to the following cycling conditions: 95° for 5 min, followed by 35 cycles of 94° for 30 sec, 62° for 30 sec, and 72° for 30 sec. After a final extension at 72° for 5 min, products were size fractionated on 3% agarose, 0.5% TBE gels. Primer sequences are listed in Table 1.

Deletion mapping: Over 50 nested deletions span the *albino* deletion complex (Russell and Russell 1959). Complementation testing between these deletions and the mutants was used to determine which deletions included *l7Rn3*. A deletion was determined to overlap the mutation if 0 albino pups were born in 30 total progeny from a cross between heterozygous mutant and hemizygous deletion animals (Rinchik *et al.* 1990). Once the deletion interval was defined, genomic DNA and cDNA probes from the region were used to delineate the extent of the deletion interval. To accomplish this, *Mus musculus* females hemizygous for the *chinchilla* allele of the *Tyrosinase* locus ($Tyr^{c\text{-}ch}$/$Tyr^{c\text{-}deletion}$) were crossed to *M. spretus* males (+^{SPT}/+^{SPT}), where $Tyr^{c\text{-}deletion}$ designates a deletion. The deletions arose on the C3Hf/Rl and 101/Rl backgrounds, but were bred to the *chinchilla* stock. Most progeny will be either $Tyr^{c\text{-}ch}$/+^{SPT} or $Tyr^{c\text{-}deletion}$/+^{SPT}. However, it was possible that the originating C3Hf/Rl or 101/Rl genome was carried across the deletion. Therefore, polymorphisms were found for the *M. musculus* (c^{ch}/c^{ch}, C3Hf/Rl and 101/Rl) and *M. spretus* (+^{SPT}/+^{SPT}) alleles by Southern analysis according to well-established techniques (Lossie *et al.* 1993). The absence of the *M. musculus*-specific fragment in DNA from $Tyr^{c\text{-}deletion}$/+^{SPT} F_1 animals indicates that a probe is deleted and therefore localized within the *l7Rn3* critical region.

Deletion interval gene annotation: We examined the annotated sequence to identify genes that were localized to the critical interval using the NCBI, University of California at Santa Cruz, and Ensembl databases (Waterston *et al.* 2002). These data were generated in part through the use of the Celera Discovery System and Celera's associated databases (Kerlavage *et al.* 2002). ESTs and mRNAs that had short stretches of homology to the *l7Rn3* domain and multiple hits across the genome were not included.

Northern blot analysis: Northern blots of polyadenylated [poly(A)$^+$] RNA from adult mouse tissues (CLONTECH, Palo Alto, CA) and whole embryos (CLONTECH) were hybridized with *Odz4* cDNAs according to standard protocols (Church and Gilbert 1984). *Odz4* was visualized using probes that span different regions of the gene (see Figure 4). Blots were stripped and reprobed with *Gapdh* as a loading and mRNA integrity control.

RT-PCR: *Odz4* RT-PCR and sequence analyses were performed on total RNA and poly(A)$^+$ RNA isolated from E7.5 to E13.5 embryos using RNAStat-60 (total RNA; TEL-TEST, Friendswood, TX) or Poly(A) Pure (mRNA; Ambion, Austin, TX). RNA was reverse transcribed with either the Superscript II or III preamplification system (Life Technologies). The resulting PCR products were electrophoresed on agarose gels, purified by QIAquick extraction (QIAGEN, Valencia, CA) or glasswool, and sequenced using an ABI377 sequencer and BigDye v3.0 chemistry (Perkin-Elmer, Foster City, CA).

***In situ* hybridization:** Embryos were recovered as described (Nagy *et al.* 2003). Embryos were fixed in 4% paraformaldehyde in PBS for 15 min to 4 hr (depending on the size of the embryo) at 4° and dehydrated through a methanol series prior to processing by previously published methods (Echelard

TABLE 1

Primers used in this study

Exon	Sequence	Exon	Sequence
1–7	ATCTGGACTCCTCCACTTGACAC	13	CCTGTCACGGAATAAAGTCTCCTT
	CTCTGGGAAGAGTTGGTGTCTTC		TCCTGCTGTTTCTGAGGTATTCTG
6–9	GTAGAACCCATACCACCCTGTTCT	14	TAATGCAAGGGATTGGTGACAG
	CTGCCGATGAGCTGGTGTAG		ATCTTCACCCTATGAGCCGTACAT
9–10	GAAGGAGAGGAAGCCCTATCG	15	CAGAGAACAGGAGTTCGGAGCTAT
	GTGAGTGTGAGGTTGGAGTTGG		GAGCTCTCTCCTTCTACCATTGGA
10–13	CCAACTCCAACCTCACACTCAC	16	ATATAATGTGCCCAGCCCACTACT
	CCTGTTCAAGGAGTTGATGGAG		CAAGGCATCTTGATACAGCCTATG
13–15	CTCCATCAACTCCTTGAACAGG	17	TTGAACTGAACTGAGGGTCTGTGT
	ATACACGGTGCTAGACGTTAGGG		GCAATCATCTGAAATGTTTCCATC
15–17	CGCTCTTCTGCACCACATCC	18	CGGCTTTGGAAGAATGAGTAGTTT
	GTCTCCCCACATCGATTTCTCC		GAAAGGCAGTTGTGAAGTGTCCTA
17–18	AGCCAAGTAGTTTATTTCCAGAGGA	19	ATGAATAATCAATTCTGCCACGTT
	ACCACTTCAGATTCTTTTCCATCA		CAATTCCAATTCCAATCATATTCA
18–23	TCTGAAGTGGTTTCATTTCTCACCA	20	AATGGTAAGACTCATCCCTTTGGA
	AGTGGCACTCGCCTCTGACA		AACAATATCCATCAGTGGACTGGAA
23–27	ACATGTTCCAGCAGGGGTGT	21	AGAATGAGCCAGTCTCAAGGATG
	AGGGTACATCTGCCATTTCCATT		CCAATAGATGCCAATCACTTTCAC
27–30	CAGATGTACCCTGGACCTGAATG	22	AACGTGCACACCATATGCTTACTT
	GGTCCCATCTGACGTCATCACT		GCACAGAGTGTGTCTCAGTGCTAA
30–32	GTGGACAAGTGATGACGTCAGAT	23	CAGTCTTCTGGCTATGACTTCTGG
	CTCAGGTAGCTCAACCTCATCTTG		GCAACTGAAAGGTAGAAACCGAAT
32–33	CCTGCAAGAGGAAATCGTCATC	24–25	CACAAACCAGCCTTTGTGAA
	AGCTTGGAGGCATCAATTTCATAG		AAGGGACCAACGACATGAAG
33–36	AGATCTGATCCTGTGGGAGAAAAG	26	TTGGCATCTGTAAACTCTCTCTGG
	GTAGTATTTGTGTGCTGGGCTGTG		AGAATGAACAGGGAGACAGGGTAG
34–37	GAGACTTCAACTACATCCGCAGAA	27	CACAGGCCTTGGATGTCACTT
	CCCAGCAAAGTGGAGATGATT		AGGAAGACACATTCATGAGGGATT
37–38	ACGTGTTGATCAAAATGGAATCAT	28	AGCATCACTGTGTTGGTATTTGGT
	CACTTGTAGTGACCTGCCTGATG		CTTATGCCTGAACTTTGGGAGTTT
38–40	GAGCTAGCCATGATGACCTACCAT	29	CCTTGGCTAAACTGCTGGTCTATT
	GTGACATTCCTCTTGCCTACAGTG		ACTTTATCTCAACCCTTGCCAGAC
40–42	GTAGGCAAGAGGAATGTCACACTG	30	TTGCAAGCACTTTACTGGCTAATC
	GGTCATTCTTGTCAAACTCGAAGA		CAGGCCTCTTGTTGATAATTGCTT
42–44	GCATCGTGCCTTTTCATCTCTAC	31	CTTGAAGCTTTCTTCCGTTTCACT
	GAGGCAAACTTCTTTGTCTCAGG		ACTCCAGCCACACATTTGTCATAG
3′ UTR	GTGGTTCCATCTTTGGCAAG	32	CCAAGGTAGAAAGTGGGTGTAGGT
	TGCATGAATTAACAATGCAACA		AAACATGCAGAACCTGTCATTGAT
D7AL7	GTAAGTGGGCTCACTGTTGTATGC	33	GAGGAATAGGTGTGATGTCACTGG
	TTGCAAACACTTAATTTCAGGACAA		GCCATTACAACAGCAGAGTAGGAG
D7Mit352	AGCCAATTGCAACCAAATTT	34	CAAATCTACAACATATTTCCAATGGTT
	AGCATGGAAAATTGACAATTCC		CTGAGGCTTTAAGGTGACTGACAT
1	CCTACAGTCAAGACAGTGGAAACC	35	CCGCATATACTTTGCTAAATCAAG
	TCTGTCACTAGACACACACCAGGA		TACTTCTCTGGTCCCTATGGGTAG
2	ACCAATCATAGCAAGTCCTTCACA	36	GTATCAGTGTCATGGCTGCTAAGT
	CCGAATGTGTCTTTAGATAGCCCT		ACAAGTGTCTCACTTTACCACAGG
3 and 4	TAATTACTTCTGGCGAAAGCAACC	37	CAGCAACCAGTGAGATCTCACCA
	CAATACACAGCATATTTCCCGAAG		CATGTCTCGTCTCACCAACTTCCTT
5	TGATAGAGTCATAAAGTGCAGCCC	38	ACTAACAGATGGCAAGGTGAGGTT
	ATTCTGCAGTTCTCTAGGGCATTT		TCTTCTCCATCAACAAGACTTTCG
6	ATGTCCACACTAGTATCCTGGCAD	39	GTACTTGGGCTCTCATTCCTTCTC
	ATCCTCTTCATCCTCCTCATCATC		TCATAGACTTTGGGAGATGATGTCTT
7	CAGACCCATTTCAGTTATCAGTGC	40	CAGATGGCAAGGTGAGGTTTGAT
	ACAACCCATTTAGTACCCAGATGC		CTATACCCACAGTGATCAAGCTTC
8	AGTTCGATGATAACCCTCATTTGT	41	GGCTTCATCTCTCTTGGATCTACC
	GAAGGGAGCACCTGTAACATTAAC		ACTCTGAACACGGTGGATTATGAA
9	GGAGTTTGTTAAGTGCAGGATAGA	42	TAATGTGTCCCTGCAGATTTGACT
	ACTAGGCAGGTGGGCTACAA		AGGAATACGGCCACAGAAGAGTAG
10	AGGATAGATTCTGGCATTTGAACC	43	ACTCATTGCTCAGGTGACTGAAAC
	CTTAAAGGTACCATCCCACTGAGG		TGCATTTATTTACAGCCTTGTTGG
11	ACATAGCACCAGCCTGTGTAGAAG		
	AAGTAATAACCCAGCCCTTTAGCC		
12	CCTCTCACCCACACAGTAATATGC		
	GAGGACCTCAGGAGAGTAATCCAG		

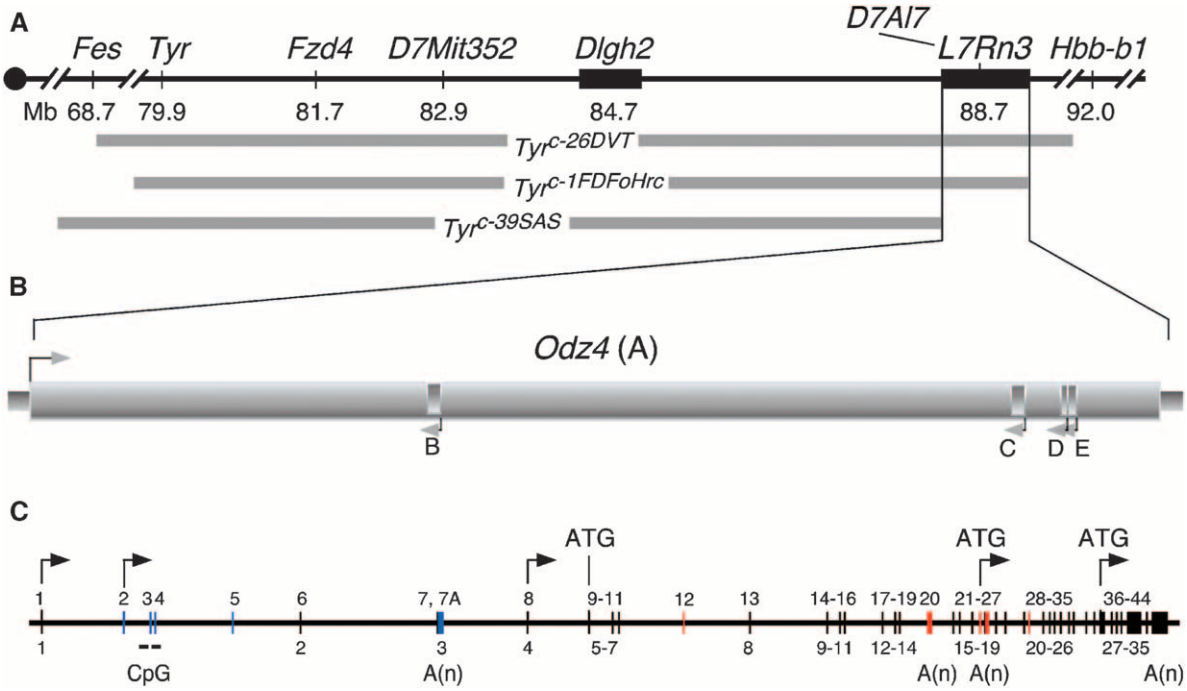

FIGURE 1.—Physical map of *l7Rn3*. (A) Physical map of *l7Rn3* in relation to the *Tyrosinase* locus. Genes and molecular markers are indicated along the 9.7-Mb region. Three nested deletions ($Tyr^{c\text{-}26DVT}$, $Tyr^{c\text{-}1FDFoHrc}$, and $Tyr^{c\text{-}39SAS}$) that span this region are depicted with the deleted intervals shaded. The endpoints of $Tyr^{c\text{-}39SAS}$ and $Tyr^{c\text{-}1FDFoHrc}$ define the critical region for *l7Rn3*. (B) Transcript map of the 0.8-Mb *l7Rn3* region. The *l7Rn3* critical region contains five expressed sequences (genes A–E). Genes A and C have an open reading frame. Gene A is also known as *Odz4*, *Odd oz homolog 4*. The longest ORF of *Odz4* predicts a 2825-amino-acid protein, while the coding region for gene C is only 133 amino acids long. Several alternatively spliced mRNAs originate from *Odz4*. These range in size from 1.5 to 12 kb. Genes B, D, and E are expressed in many different tissues and at different timepoints during development, but do not contain significant ORFs. (C) The *Odz4* gene. Black vertical lines represent previously identified *Odz4* exons, with the original nomenclature indicated at the bottom. The new exon numbers are located on top of the horizontal bar depicting the *Odz4* genomic locus. Blue vertical lines represent newly identified exons that do not change the protein coding sequence, while red vertical lines are new exons that are predicted to change the protein structure. Arrows indicate transcriptional start sites, and ATG sites are indicated. The map locations of *Fes*, *Tyr*, *Frizzled 4* (*Fzd4*), *Discs large homolog 2* (*Dlgh2*), and *Hbb-b1* are shown.

et al. 1993). Digoxygenin-labeled antisense probe was generated according to the manufacturer's instructions (Boehringer Mannheim, Indianapolis).

RESULTS

Deletion mapping and candidate gene identification: Over 50 nested deletions span the 24-Mb *Tyrosinase* deletion complex, which extends from the *Feline sarcoma oncogene* (*Fes*) to the *Hemoglobin beta chain 1* (*Hbb-b1*) locus on mouse chromosome 7 (RUSSELL 1989). The *l7Rn3* complementation group lies 9.7 Mb distal to *Tyrosinase* within this complex, and three of the deletions are depicted here (Figure 1A). Six phenotypically distinct ENU-induced mutations define the *l7Rn3* locus (RINCHIK and CARPENTER 1999). Five of these mutant lines (*m1*, *m3*, *m4*, *m5*, and *m6*) were propagated in our laboratory for further analysis. The *m2* mutants have a phenotype that is similar to the *m1* mutants and were not included in these studies. Two molecular markers in this region, *D7Mit352* and *D7Al7*, were used for genotyping. Previous studies showed that all of the *l7Rn3* mutant lines failed to complement the $Tyr^{c\text{-}26DVT}$ and $Tyr^{c\text{-}1FDFoHrc}$ deletions (RINCHIK and CARPENTER 1999). Further complementation studies in our lab between the four lethal mutant lines (*m1*, *m3*, *m4*, and *m5*) and the nested deletions demonstrate that the $Tyr^{c\text{-}39SAS}$ deletion complements our mutants (data not shown). Therefore, the *l7Rn3* allele series is located between the breakpoints of the $Tyr^{c\text{-}39SAS}$ and the $Tyr^{c\text{-}1FDFoHrc}$ deletion regions (Figure 1A).

One method utilized at the University of California at Santa Cruz to integrate the transcriptome with the computer-based exon prediction programs is SGP, which compares mRNA sequences and spliced ESTs to identify the most likely gene boundaries in a given region (KAROLCHIK *et al.* 2003). This algorithm requires at least 97.5% identity for inclusion, eliminates small blocks of sequence, aligns the transcripts according to predicted splice junctions, and merges overlapping blocks into clusters. SGP analysis predicts that five genes are located within the 700-kb domain encompassing *l7Rn3* (Figure 1B; Table 2, SGP column). The largest of these, *Odz4*, spans the entire critical region (Figure 1, A and B). The

TABLE 2

Summary of the transcripts identified in the 12-Mb domain

Figure 1 gene	Gene	SGP evidence	Mouse mRNAs	Spliced mouse ESTs	Human mRNAs	Human/mouse homology
A	*Odz4*	chr7.1260	AF059485 AB025413 AK031375 CG672227 AK053790 AK039472 AK078539 AK122490 D87034 AK054459	Numerous	AB037723 AK056531 AL080120 AK023935	chr7_1642.1 chr7_1645.1 chr7_1650.1 chr7_1651.1 chr7_1652.1 chr7_1653.1 chr7_1654.1
B		chr7.1261	AK035005 AK020195 AK053915	BY707033		
C		chr7.1262	AK077305	BB617637		
D		chr7.1263		BB862371		
E		chr7.1264		BB861794		

The predicted genes (SGP and human/mouse homology), as well as identified mRNAs and ESTs, are indicated.

other "genes" were predicted on the basis of evidence from a single mouse EST clone (Table 2; Figure 1B, genes B–E). We excluded ESTs and mRNAs that had incomplete stretches of homology and multiple hits across the genome, as this "hybridization" pattern is indicative of a repetitive element or short protein domain.

Annotation of the *Odz4* genomic locus: The *Odz4* locus is very complex. Many mRNAs, ESTs, and predicted transcripts lie within this 735-kb domain. To determine which of these encode unique genes, we compiled RT-PCR data from each of the annotated exons to determine its expression profile in early postimplantation embryos as well as in adult tissues.

Eight mouse and four human mRNAs delineate the *Odz4* gene (Table 2). These include three RIKEN cDNAs (AK031375, AK053790, and AK039472) that partially overlap *Odz4*, a RIKEN clone that denotes an alternative 3′ UTR for *Odz4* (exon 20; AK078539), two mouse (D87034 and AK122490) and three human *ELM2* (*Expressed in low-metastatic cells*; AB037723, AL080120, and AK023935) sequences, a human *ODZ4* transcript (AK056531), as well as two known *Odz4* cDNAs (AF059485 and AB025413; Wang *et al.* 1998; Oohashi *et al.* 1999). The positions of these exons were determined by BLAST alignment with the mouse genome.

The full-length *Odz4* gene is predicted from two overlapping mouse cDNAs (AF059485 and AB025413; Wang *et al.* 1998; Oohashi *et al.* 1999). Although these transcripts have slightly different cDNAs, they predict the same basic protein structure (Figure 2A). Since no two cDNAs are identical, we predicted that different tissues and developmental stages would have unique *Odz4* messages. We also postulated that there could be different protein isoforms that correlated with these temporal and spatial transcripts.

We identified five new alternatively spliced exons that are located upstream of the start codon (Figure 1C, blue exons 2, 3, 4, 5, and 7A). These exons undergo extensive alternative splicing and use three different promoters. It is likely that the different promoters confer tissue-specific expression patterns, as transcripts originating from exon 1 are detected in multiple tissues and stages of development, while mRNAs starting from exon 2 display three distinct expression patterns. Amplification products between exons 2 and 6, 7, or 15 are found only in adult brain, while RT-PCR between exons 2 and 13 indicates that this amplicon is expressed only in adult ovary (Figure 3B) and E11.5 embryos. However, RT-PCR products that contain exon 2–6, 22, 24, 30, 31, 32, 33, and 34 are observed in most tissues. No amplification products are obtained between exon 1 and exon 2, suggesting that these exons are alternative transcriptional start sites for *Odz4*.

Two additional upstream exons are encoded by the 2.5-kb AK031375 transcript (Figure 1C, exons 3 and 7A). This full-length message was isolated from E13.0 testis, includes exons 3, 6, and 7A, and introduces an intragenic poly(A) signal. A large CpG island overlaps exon 3, which indicates that it could be used as another transcription start site. In addition, RT-PCR amplification between exons 1 and 7 indicates that there are three major amplicons in most tissues (Figure 3C). The smaller fragments harbored different combinations of exons 1–6, although none of these alternatively spliced products contained exon 2.

We identified five alternatively spliced exons (12, 20, 24, 25, and 29 shown in red) that could generate multiple protein isoforms (Figure 1C; InterProScan; Zdobnov and Apweiler 2001). Exon 12 (Figure 1C, Table 2, chr7_1650.1) is detected only in the adult brain (Figure

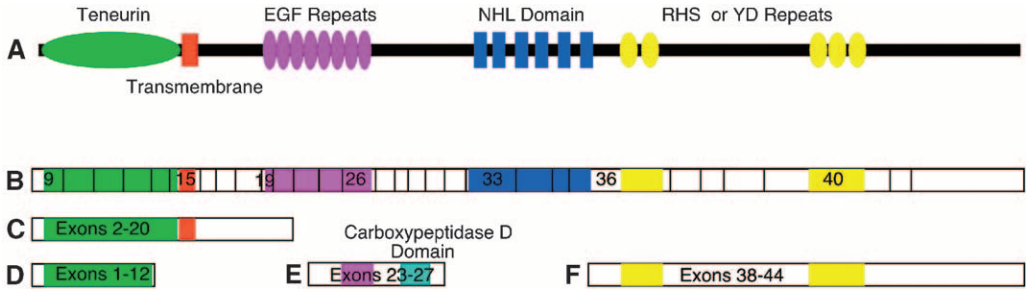

FIGURE 2.—Alternative splicing predicts five different ODZ4 protein isoforms. (A) Overview of the full-length protein predicted from cDNA AF059485. The black bar represents the entire protein, with domains indicated by different colored regions. Protein prediction models indicate that the Teneurin domain (green oval) is intracellular, while the EGF-like (epidermial growth factor-like) repeats (fuscia ovals), NHL (NCL1, HT2A, and LIN41 consensus protein domain; blue rectangles), and RHS repeats (yellow ovals) are extracellular. (B) The locations of the exons encoding specific protein domains are indicated by vertical black bars, and numbered when transitions are present. (C) Protein predicted from an RT-PCR product amplified from exons 2 to 20 (AK078539). (D) Protein predicted from an amplicon between exons 1 and 12. (E) Protein predicted from two eye cDNAs (AK053970 and AK039472). This protein would encode an entirely new protein with one EGF-like domain and a carboxypeptidase D domain. (F) Protein predicted from two 3′ cDNAs (AB037723 and AL080120), which can be produced from an internal promoter.

3A) and is predicted to result in a truncated protein that contains a partial Teneurin N intracellular domain (Figure 2D).

The 1.7-kb cDNA encoding exon 20 (Figure 1C; AK078539) was isolated from tissue surrounding the Mullerian duct of an E12.0 female embryo. RT-PCR indicates that this exon is expressed at low levels in adult brain and in the embryo (data not shown). Exon 20 contains many translation stop codons and does not appear to harbor any known protein domains. *In silico* examination indicates that an alternative poly(A) site is located within the first 450 bp of this exon. Protein prediction software indicates that the short protein isoform will include the Teneurin N intracellular domain and the transmembrane domain (Figure 2C; ZDOBNOV and APWEILER 2001).

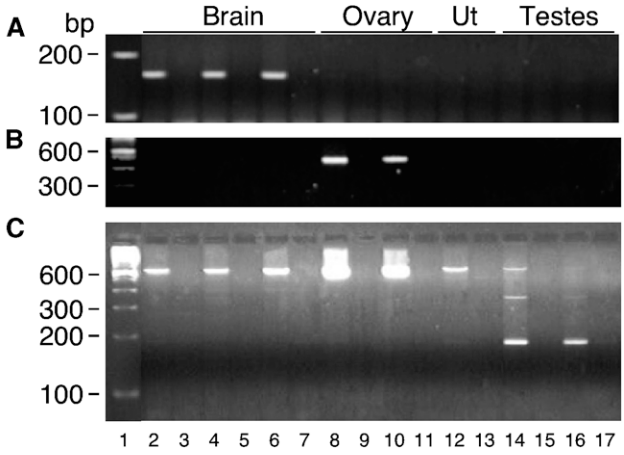

FIGURE 3.—RT-PCR demonstrates tissue-specific expression of *Odz4*. (A) Lanes 2–7. This RT-PCR product between exons 6 and 13 is detected only in adult brain. (B) Lanes 8–11. In the adult, a transcript between exons 2 and 13 is expressed only in the ovary. (C) Lanes 2–17. An amplicon between exons 25 and 29 is expressed in every tissue examined and contains two testis-specific transcripts. Even lanes, (+) RT; odd lanes, (−) RT. Ut, uterus.

Exons 24 and 25A were identified from two eye cDNAs (AK053790 and AK039472). These transcripts overlap to produce two additional noncoding *Odz4* exons that are alternatively spliced in testis (Figure 3C). AK039472 is predicted to produce a novel protein that would be a short, secreted peptide with three EGF repeats and a carboxypeptidase D domain (Figure 2E). The other eye cDNA does not predict any significant protein isoforms.

Two human *ELM2* cDNAs (AB037723 and AL080120) have ~90% identity to the murine *Odz4* gene. These transcripts overlap the last eight exons of *Odz4* to create an additional 4 kb of 3′ UTR. Protein prediction programs predict that these transcripts will produce a secreted form of ODZ4 that contains only an RHS domain (Figure 2F). RHS domains were first identified in bacteria, and members of the TEN/ODZ protein family are the only vertebrate proteins known to have this type of protein domain.

A crossover eliminates other cDNAs and ESTs as candidates: Eight small mRNAs and ESTs that do not encode alternatively spliced products of *Odz4* are located within the 735-kb genomic locus (Table 2). Some of these are transcribed in the same orientation as *Odz4*, while others are predicted to be expressed from the opposite strand. Four expressed sequences were predicted by SGP analyses to encode genes within the *Odz4* locus (Figure 1B, genes B–E; Table 2). Only one of these sequences, gene C, contains a significant ORF. Gene C (SGP Chr7.1262; AK077305; BB617637; BB020862) is 1.9 kb in length and spans four exons. It was isolated from an adult pituitary gland, and the predicted protein is 133 amino acids in length.

While examining hemizygous animals for phenotype characterization, we encountered two animals with a BALB/cRl genotype (*i.e.*, *m1*/deletion) at *D7Mit352*, which is located 1 Mb upstream of the *Odz4* locus. Since these animals were viable, they must have contained a recombination event between *D7Mit352* and the *m1* mutation. Further analysis at several polymorphic mark-

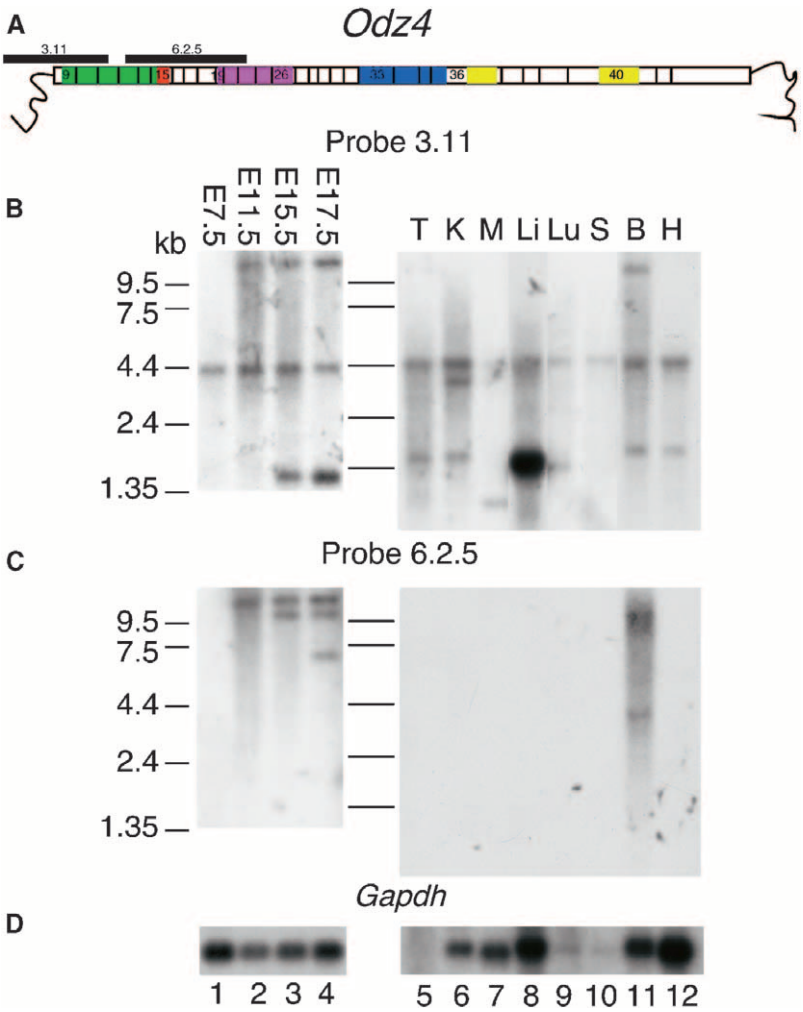

FIGURE 4.—Northern analysis of *Odz4*. (A) Representation of the *Odz4* cDNA. (A) The two cDNA probes used for Northern analysis (3.11 and 6.2.5). The 3.11 probe consists mostly of 5′ UTR with some protein coding sequence, while the 6.2.5 probe is derived entirely from the coding region. (B) Developmental and adult expression of 5′ *Odz4*. During embryogenesis, a 4.5-kb *Odz4* transcript is the first to appear, which is detected by this probe throughout embryonic development and into the adult stage. The large 12-kb mRNA is first detected at E 11.5. Although this message is detected throughout embryogenesis, it is silenced in the majority of adult tissues, with the exception of the brain. The 2.0-kb transcript is detected during midgestation and persists in most tissues through adulthood. However, it is the predominant transcript detected in the liver. In addition, adult kidney and heart show additional alternatively spliced products. (C) The *Odz4* coding region shows different expression patterns. Using a probe that spans the transmembrane domain and will hybridize to both intracellular and extracellular regions of *Odz4*, we demonstrate that the protein-coding region has significantly different expression patterns. A 12-kb mRNA is detected first, with a 10-kb transcript appearing by E11.5. By late gestation, we also detect a 6.5-kb message. There is no evidence that this probe detects the 4.5- and 2.0-kb transcripts. There is also a very different expression profile in the adult. In the brain, a large band corresponds to the 10- and 12-kb mRNAs. In addition, the 4.5-kb transcript is also detected. At this exposure (24 hr), no transcripts are detected in other tissues. A longer exposure indicates that the 10- and 12-kb transcripts are detected in testes, kidney, and heart (data not shown). (D) *Gapdh* was used as a loading and mRNA integrity control. The following tissues and embryonic timepoints were used for analysis: embryonic day 7.5 (E7.5), E11.5, E15.5, E17.5, testes (T), kidney (K), skeletal muscle (M), liver (Li), lung (Lu), spleen (S), brain (B), and heart (H).

ers located across the *Odz4* gene indicated that the recombination occurred proximal to *Odz4* in one of the progeny, but distal to *Odz4* exon 9 in the other animal (data not shown). These data demonstrate that the *m1* mutation occurs distal to exon 9 and eliminates all of the upstream genes as candidates for the *l7Rn3* allelic series.

Northern analysis of *Odz4*: Northern analyses using two probes from different regions of the gene detect multiple patterns of *Odz4* expression that vary depending on tissue type and stage of development. Embryonic expression using a probe from the 5′ end of *Odz4* demonstrates that a 4.5-kb message is detected by E7.5 (Figure 4A, probe 3.11). As embryogenesis progresses, a 12.0-kb transcript is seen by E11.5, and all of the three major *Odz4* isoforms are active between E15.5 and E17.5. However, in most adult tissues (testes, liver, lung, and heart) this probe detects only the 4.5- and 2.0-kb transcripts, indicating that this 12-kb message is primarily embryonic. The liver and brain have unique expression profiles in the adult animal. A 2.0-kb transcript is exceptionally abundant in the liver, while all three major transcripts are readily detected in the brain. In addition, alternative splicing is apparent in these tissues, as the kidney and skeletal muscle show unique *Odz4* transcripts. This probe contains exons 6–11 and includes 5′ UTR, as well as part of the Teneurin N intracellular domain.

A probe from the middle portion of the gene (probe 6.2.5) shows a much different pattern of expression. This probe contains exons 13–21 and sequence for part of the Teneurin N intracellular domain and the tenascin-like EGF-like repeats. Although a 12.0-kb transcript is detected with this probe in the same developmental timescale as the 3.11 probe, the 4.5-kb message is not observed (Figure 4B). However, the 6.2.5 probe also

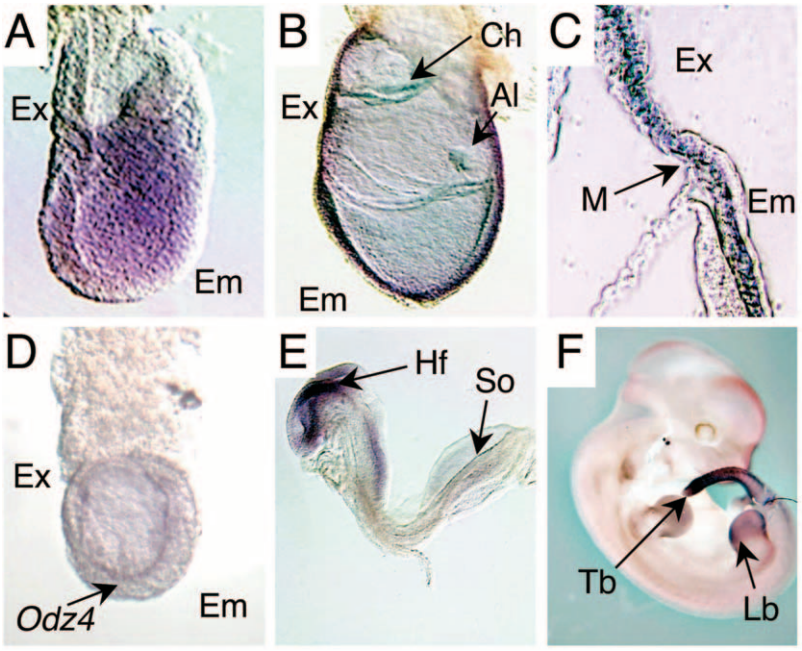

FIGURE 5.—Whole-mount *in situ* hybridization of *Odz4*. We used a probe corresponding to nucleotides 148–946 of *Odz4* for these experiments (OOHASHI *et al.* 1999). This region overlaps the Teneurin intracellular protein domains. These experiments were performed in wild-type embryos (A, B, C, E, and F) and *m1* mutant (D) embryos. (A) Gastrulation stage. *Odz4* is expressed in a gradient in the epiblast of E6.5 embryos. (B) By E7.5, expression is confined to the mesodermal layer of the embryonic and extraembryonic tissues. (C) Magnification of the transition between the embryonic and extraembryonic regions. *Odz4* expression is restricted to the mesoderm in embryonic and extraembryonic lineages. (D) Expression of *Odz4* in *m1* mutants. At E8.5, *Odz4* demonstrates weak expression in the epiblast of *m1* mutants. When compared to E6.5 embryos (A), it is clear that the *m1* mutants have markedly reduced expression of *Odz4*. (E) *Odz4* expression at E8.5. *Odz4* expression is abundantly expressed in the developing head folds. In addition, there is weak expression in the posterior somites and presomites. (F) Expression of *Odz4* in midgestation. By E11.5, *Odz4* is expressed in rapidly dividing tissues, such as the tail bud and limb. The embryonic (Em), extraembronic (Ex), mesoderm (M), allantois (Al), chorion (Ch), head folds (Hf), somites (So), tail-bud (Tb), and limb-bud (Lb) regions are indicated.

hybridizes to a 7.0-kb transcript (E17.5) and a 10.0-kb *Odz4* mRNA later in development (E15.5 and E17.5). In the adult, this probe primarily detects brain-specific transcripts of 12.0, 10.0, and 4.5 kb. Longer exposures indicate weak expression of the 12.0- and 10.0-kb messages in testes, kidney, and heart (data not shown). Northern data using a probe from the 3′ end of *Odz4* show a similar expression pattern to probe 6.2.5 (data not shown). The differences in expression patterns between the 5′ UTR/amino terminal and coding region probes indicate that *Odz4* is subject to complex transcriptional regulation, generating multiple mRNA products that are active during specific embryonic and adult time points.

Dynamic expression of *Odz4* during embryogenesis: Since Northern analysis shows that *Odz4* could have tissue-restricted patterns of expression, we examined its expression early in development using whole-mount *in situ* hybridization of normal, as well as *m1* mutant, embryos. We found that *Odz4* is ubiquitously expressed in the epiblast and extraembryonic regions as early as E6.5 (Figure 5A). However, this expression is weak and was observed only after an overnight incubation. By E7.5, *Odz4* is highly expressed in the mesoderm of the developing embryo and extraembryonic tissues (Figure 5, B and C). At E8.5, *Odz4* is expressed mainly in the neural ectoderm (Figure 5E), while expression in older embryos (E 11.5) is confined to the tail bud and limbs (Figure 5F). Analysis of *m1* mutant embryos at E8.5 (Figure 5D) demonstrates that expression of *Odz4* is markedly reduced compared to age-matched (Figure 5B) or E6.5 (Figure 5A) embryos.

Phenotypes of the *l7Rn3* mutant alleles: We established the time of death and the appearance of developmental landmarks that are associated with each of the *l7Rn3* mutants to determine if the phenotypes correlated with the *Odz4* expression patterns. The most severe allele, *m1*, arrests at E6.5 with a phenotype reminiscent of a pregastrulation stage embryo (Figure 6, A and B; Table 2). Mutants are resorbed by E9.5, do not produce embryonic or extraembryonic mesoderm, arrest before primitive streak formation, and lack a morphological A-P axis (H. NAKAMURA and M. J. JUSTICE, unpublished results). Animals homozygous for the *m2* allele have a phenotype that is similar to the homozygous *m1* mutants (data not shown). Phenotypic and mutational analysis of the *m2* allele was not pursued.

The *m3/m3* homozygotes, which demonstrate developmental delay by E7.5, undergo gastrulation, generating mesoderm in embryonic and extraembryonic regions to establish an A-P axis (Figure 6, C and D). These mutants die later than the other alleles (between E9.5 and E11.5) with open head folds, kinky open neural tubes, and incomplete somitogenesis (Table 3). The *m4/m4* mutants demonstrate a gradual delay in embryogenesis that is first evident at E5.0. By E8.5, *m4/m4* homozygotes lag behind by 1 full day compared to normal littermates. Although *m4/m4* homozygotes initiate head-fold elevation, the embryos fail to elongate and appear to have general mesodermal defects that cause

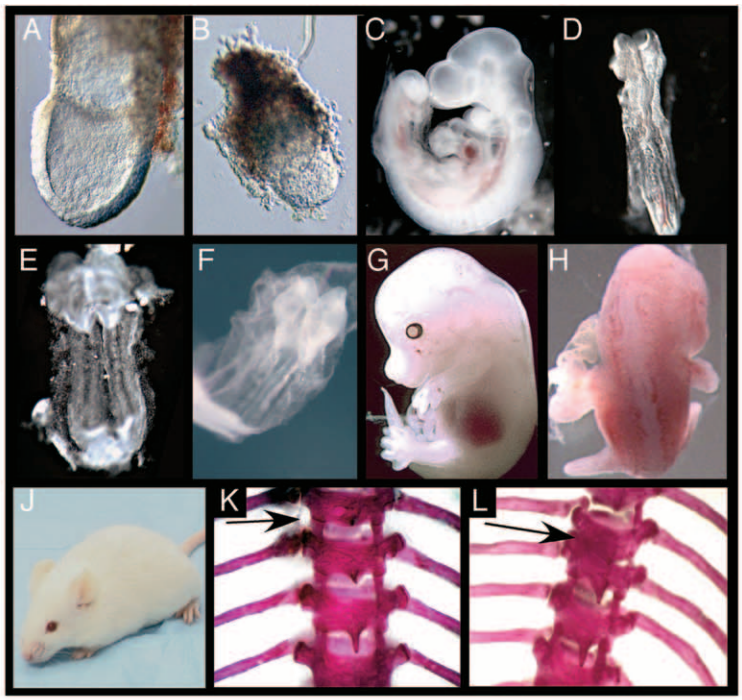

Genotype	Neural Tube Closure Anterior	Neural Tube Closure Posterior	Somite Number	Heart	Sensory Placode Optic	Sensory Placode Otic
+/+ (E7.5)	-	-	0-2	crescent shaped	-	-
+/+ (E9.5)	+	+	22-30	advanced loop/adult	+	+
l7Rn3 $^{m1/m1}$ (E7.5)	-	-	0	not formed	-	-
l7Rn3 $^{m3/m3}$ (E9.5)	-	-	20-25	looped	+	+
l7Rn3 $^{m4/m4}$ (E9.5)	+	-	3-6	none	-	-
l7Rn3 $^{m5/m5}$ (E9.5)	+	+/-	5-10	round shaped	+	+

Genotype	N	T6/T7 or L3/L4 Fusion	Abnormal C2 Process
l7Rn3 $^{Del(Tyr)c\text{-}26DVT/m6}$	10	0 %	60 %
l7Rn3$^{m6/m6}$	10	20 %	40 %
l7Rn3$^{m3/m5}$	11	27 %	18 %
m/+	26	0 %	1 %
+/+	20	0 %	0 %

m indicates *l7Rn3* ^{m3}, *l7Rn3* ^{m5}, *l7Rn3* ^{m6} or Del(*Tyr*) $^{c\text{-}26DVT}$

FIGURE 6.—Phenotypes of the *l7Rn3* mutants. (A) Wild-type animal at E6.5. (B) *m1/m1* mutants are delayed compared to normal littermates and have not started to undergo gastrulation by E6.5. (C) Normal E9.5 embryo. (D) *m3/m3* embryo at E9.5. Compared to normal control, the *m3* homozygotes demonstrate developmental delay with incomplete fusion of the neural tubes. The neural tubes are also misformed. (E) Compared to control embryos, *m4/m4* homozygous mutants are severely delayed at E9.5. They also show incomplete somitogenesis and are not able to undergo cardiogenesis. (F) *m5/m5* mutants are also delayed at E9.5 compared to control animals. They also have defects in somite formation and heart development that are less severe than those in the *m4/m4* animals. (G) Control animal at E13.5. (H) *m6* lethal animals ($l7Rn3^{m6}/Tyr^{c\text{-}26DVT}$) die during midgestation with a variety of phenotypes, including defects in turning, neural tube abnormalities, vascularization problems, and limb-bud malformations. (J) The reciprocal cross ($Tyr^{c\text{-}26DVT}/l7Rn3^{m6}$) produces viable animals that have subtle skeletal abnormalities. (K) Skeletons from control animals. (L) The T6 and T7 vertebrae are fused in $Tyr^{c\text{-}26DVT}/l7Rn3^{m6}$ animals. A summary of the phenotypes depicted is shown (bottom).

uncoordinated somite segregation (Figure 6, C and E; Table 3). Although a rudimentary allantois forms in the *m4* mutants, it makes only a partial fusion with the chorionic plate, which most likely leads to embryonic failure between E9.5 and E11.5.

Animals homozygous for the *m5* allele show a delay in embryonic development that is similar to the *m4* mutants. However, they progress slightly further in development than the *m4* allele and are able to initiate heart formation. Like the *m4* mutants, the allantois in the *m5/m5* homozygotes fails to grow and does not fuse with the chorion, resulting in death between E9.5 and E11.5 (Table 3; Figure 6, C and F).

The *m6* allele demonstrates two distinct phenotypes, which range from embryonic lethal to fully viable, depending upon which parent transmits the mutated chromosome (Figure 6, G and H). Two conditions must be met for the severe phenotype to be observed. First, the *m6* mutation must be transmitted from the mother. Second, the paternally inherited allele must be deleted

TABLE 3

Time of death of the *Odz4* mutants

Cross	Genotype	Embryonic day 6.5	7.5	9.5	10.5	11.5	12.5	13.5	14–15	16–17
m1/+ × m1/+	+/+	4	8	4	5	3				
	m1/+	10	18	8	7	7				
	m1/m1	5	9	1	0	0				
	Resorbed	2	0	3	5	4				
	mut + res/total	7/21	9/35	4/16	5/17	4/14				
	% mutant or resorbed	**33**	**26**	**25**	**29**	**29**				
m3/+ × m3/+	+/+		6	27	9	2				
	m3/+		15	47	17	4				
	m3/m3		7	21	2	0				
	Resorbed		0	3	6	3				
	mut + res/total		7/28	24/98	8/34	3/9				
	% mutant or resorbed		**25**	**25**	**24**	**33**				
m4/+ × m4/+	+/+	8	15	36	18	6				
	m4/+	14	31	70	39	15				
	m4/m4	10	14	30	4	0				
	Resorbed	0	1	6	13	3				
	mut + res/total	10/32	15/61	36/142	17/69	3/24				
	% mutant or resorbed	**31**	**25**	**25**	**25**	**13**				
m5/+ × m5/+	+/+	2	18	23	8	7				
	m5/+	5	34	49	8	13				
	m5/m5	1	21	19	4	0				
	Resorbed	1	0	6	4	4				
	mut + res/total	2/9	21/73	25/97	8/24	4/24				
	% mutant or resorbed	**22**	**29**	**26**	**25**	**17**				
m6/+ × Δ/+	+/+ or m6/+			51	25	16	14	14	17	25
	m6/m6			13	6	3	2	2	2	2
	Resorbed			1	3	1	1	3	3	0
	mut + res/total			14/65	9/34	4/20	3/17	5/19	5/22	2/27
	% mutant or resorbed			**22**	**27**	**20**	**18**	**26**	**23**	**7**

The crosses, predicted genotypes, and results are indicated. The *m1* mutants die before E9.5, while the *m3*, *m4*, and *m5* homozygotes live until E10.5. The *m6* lethal allele dies between E8.5 and E14.5.

for the *Odz4* critical region (*i.e.*, these animals must have a *m6/Tyr$^{c\text{-}26DVT}$* genotype). These embryos die between E8.5 and E17.5 and have a broad range of phenotypes, which include developmental delay and kinky neural tubes (Figure 6, G and H; Table 3). In addition, some show clear abnormalities in vascularization and limb bud elongation. When the *m6* mutation is transmitted from the father, a much different phenotype is observed. These animals survive to adulthood and many appear normal, although ~30% are runted and scruffy at weaning. In addition, these mutants have skeletal abnormalities, which are discussed below.

Together, these data would suggest that *m1* represents a loss-of-function allele and that the *m3*, *m4*, *m5*, and *m6* alleles are hypomorphic mutations. To test this possibility, we examined the embryonic phenotype of compound heterozygotes (Table 4). Previous data showed that each of the *m2*–*m6* alleles fail to complement *m1* (Rinchik and Carpenter 1999). With the exception of the *m1/m3* animals, all heterozygotes compound with *m1* demonstrate the phenotype of the less severe allele, suggesting that these alleles are hypomorphic. When compound heterozygotes are formed by mating either *m1/+* or *m4/+* animals with *m3/+* heterozygotes, the double mutants show a phenotype that is reminiscent of the more severe *m1* or *m4* phenotype. However, in matings with *m5/+* heterozygotes, the *m3/m5* compound heterozygotes are viable.

We examined the viable mutants (*m3/m5*, *Tyr$^{c\text{-}26DVT}$/m6*, and *m6/m6*) and found that subtle skeletal abnormalities occur in both the *m3/m5* compound heterozygotes and the *m6/m6* or deletion/*m6* viable animals (Figure 6, J and K). An aberrant spinous process of the C2 vertebrae occurs in 60% of the compound *m3/m5* heterozygotes, while 40% of *m6/m6* homozygous and 18% of *Tyr$^{c\text{-}26DVT}$/m6* hemizygous mutants display this pheno-

TABLE 4

Complementation analysis of allelic embryonic phenotypes

	Phenotypes of compound heterozygotes			
Parents	*m1*/+	*m3*/+	*m4*/+	*m5*/+
m1/+	m1	m1	m4	m5
m3/+	m1	m3	m4	Viable[a]
m4/+	m4	m4	m4	m5
m5/+	m5	Viable[a]	m5	m5

The stage of death and phenotype are presented as similar to a given allele or viable. Compound heterozygotes between *m1* and *m4* or *m5* animals show the less severe phenotype, while *m1*/*m3* compound heterozygotes demonstrate the more severe phenotype observed with *m1*. In crosses between *m3* and *m4*, the more severe phenotype is also observed.

[a] Skeletal defects; see Figure 6.

type. Twenty percent of the *m6/m6* homozygous mutants and 27% of the $Tyr^{c\text{-}26DVT}$/*m6* hemizygous mutants also display fused T6/T7 thoracic or L3/L4 lumbar vertebrae (Figure 6). These fusions are not detected in the *m3*/*m5* compound heterozygotes.

Mutation analysis: To identify the ENU-induced lesions, we sequenced RT-PCR products from homozygous mutants. Overlapping amplicons from the *Odz4* coding region were sequenced directly. We identified a G-to-C transversion that causes an Ala 2642 to Pro missense mutation in the *m4* allele (Figure 7). This mutation occurs in the globular region of the C terminus, which is predicted to be involved in ligand binding (Oohashi *et al.* 1999). This amino acid appears to be important evolutionarily, as it is conserved among all four members of the mouse ODZ proteins, as well as in the human ODZ1, Drosophila TENA, rat NEURESTIN, chicken TENEURIN 1, and zebrafish TENM4 proteins. We sequenced genomic DNA from heterozygous animals in an attempt to identify the remaining mutations. However, we did not find mutations in the coding sequence of *m1*, *m3*, *m5*, or *m6*. It is possible that these mutations lie in unidentified exons or regulatory elements or that the sequencing of heterozygous DNA did not reveal these lesions.

DISCUSSION

We report here that mutations in *Odz4* are responsible for the *l7Rn3* allele series. This conclusion is based on the following criteria: (1) *Odz4* maps to the *l7Rn3* critical region; (2) the large size and complex transcriptional regulation of *Odz4* explains the phenotypic diversity observed within the *l7Rn3* allele series; (3) *Odz4* is expressed before or during the developmental time points at which the phenotypic anomalies are manifested; and (4) we find mutations within and/or defects in expression of *Odz4* in two of the *l7Rn3* alleles.

While generating the *l7Rn3* mutants, Rinchik found 31 alleles that formed 10 complementation groups along the *Tyrosinase* deletion complex (Rinchik and Carpenter 1999). Seven mutants clustered within the 7.1-kb *Myosin heavy chain VIIa* (*Myo7a*) gene (Gibson *et al.* 1995). In contrast, only three alleles were isolated from the 2.0-kb *Embryonic ectoderm development* (*Eed*) gene (Rinchik and Carpenter 1999). Since the *l7Rn3* complementation group contained six mutations, we proposed that the causative gene would produce a relatively large mRNA. After narrowing the critical region for *l7Rn3* to an ~700-kb domain, it was evident that that *Odz4* was the best candidate gene. The 9.7-kb *Odz4* transcript spanned the entire domain and was the only large protein-coding gene found in the *l7Rn3* critical region.

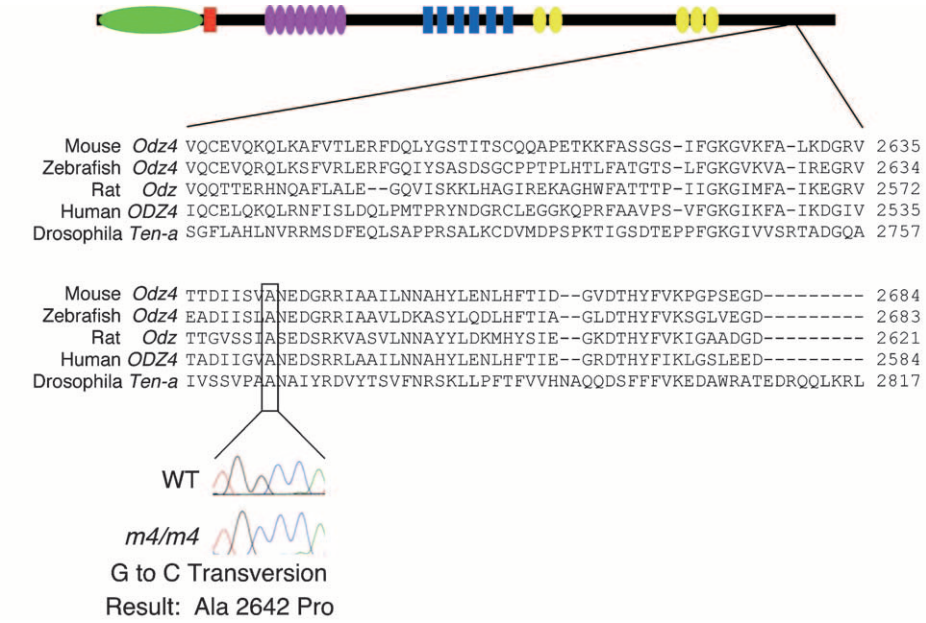

Figure 7.—Mutation analysis identified a mutation in the *m4* allele. Sequence analysis of RT-PCR products identified an Ala 2642 Pro mutation in the *m4* allele. This mutation resides in the globular domain in the C terminus in an amino acid that is conserved among all mouse homologs and in Drosophila Ten[a], but not Ten[m].

Our current studies demonstrate that the previously identified *Odz4* exons (Wang *et al.* 1998; Oohashi *et al.* 1999) have a broad expression pattern and are detected in most adult and embryonic tissues. However, some of the newly discovered *Odz4* exons are expressed in complicated developmental and tissue-specific patterns. The most striking example is exon 2, which is part of at least three distinct *Odz4* transcripts. Initial evidence revealed that exon 2 was not coamplified with exon 1, indicating that these two 5′ UTR exons are alternative transcriptional start sites for *Odz4*. Further investigation demonstrated that exon 2 is ubiquitously expressed in most transcripts. However, in two alternatively spliced messages exon 2 is detected only in adult brain or in ovary and E11.5 embryos. Similar expression profiles are seen with the other newly identified *Odz4* exons. Taken as a whole, these data support our hypothesis that *Odz4* uses multiple enhancer elements and alternative start sites to direct its complex tissue-specific and developmental expression profiles.

What is the purpose of all of these different transcripts? One possibility is that they increase the protein diversity of ODZ4. Alternative splicing, along with the use of multiple polyadenylation sites, is one method that mammalian genes can use to maximize the protein function and tissue distribution (Boue *et al.* 2003). In addition, different tissue types could easily express specific transcripts by using alternative splicing of various cassettes of exons that would be best suited to that tissue (Lee and Irizarry 2003). This is an intriguing possibility, as exons that encode the tenascin-like EGF-like repeats have conserved intron/exon structure among several of the different *Odz* orthologs (Minet and Chiquet-Ehrismann 2000). Furthermore, some of the *Odz4* mRNAs lack the characteristic EGF-like repeats, indicating that they can be spliced in cassette form.

Hundreds of pockets of high homology between mouse and human lie along the entire *Odz4* genomic locus (Karolchik *et al.* 2003). These regions lie in discrete portions of sequence and most are located within introns. It is probable that these short domains of high human/mouse homology harbor regulatory elements that are crucial for establishing the correct temporal-spatial expression pattern of the many *Odz4* transcripts (Hardison 2003). ODZ4 also has several RHS/YD repeats located in the C-terminal region of the protein. Although these elements are prevalent in prokaryotes, in eukaryotes, they are found only in ODZ family members (Minet and Chiquet-Ehrismann 2000). In prokaryotes, there are three RHS subfamilies, and new members are generated by intermolecular recombination between different family members (Zhao and Hill 1995). It is possible that ODZ protein diversity is increased by RNA-RNA *trans*-splicing events among the four ODZ homologs. *Trans*-splicing, which occurs when two different mRNAs recombine to generate a chimeric cDNA, has been recently detected in mammals (reviewed in Fedorova and Fedorov 2003). This is an interesting idea, given that two chimeric cDNAs that include *Odz4* have been identified in mouse and human (Liu *et al.* 1999; Adelaide *et al.* 2000). It is clear from our expression studies that many different ODZ4 protein isoforms can be generated from alternative splicing of *Odz4*, and it is likely that this is a major mechanism for maximizing the diversity of partners with which ODZ4 can interact during development.

Developmental expression of *Odz4* occurs in a spatiotemporal pattern that mimics the defects seen in the *l7Rn3* complementation group. *Odz4* is ubiquitously expressed at E6.5, but is restricted to the mesoderm by E7.5. At E6.5, the *m1* mutants are smaller than their wild-type littermates and have not started to gastrulate. By E7.5, the embryos are markedly delayed, have not begun to gastrulate, and are unable to develop beyond this point. Each of the other mutant alleles also demonstrates developmental delay, indicating that gastrulation may be impaired in all members of the *Odz4* allelic series. One reason for their developmental delay could be that they have mutations that affect cell proliferation and/or cell death, which could alter gastrulation. In this scenario the null mutants (*i.e.*, *m1*) would be unable to progress through gastrulation because they completely lack the ODZ4 isoform(s) that is crucial for mesoderm induction. We predict that the hypomorphic alleles would have partially functional ODZ4 protein isoforms or low levels of ODZ4 protein that could overcome this block at gastrulation. However, these hypomorphic mutants would subsequently fail when other underlying biological processes required different ODZ4 protein products. Since ODZ4 forms homo- and heterodimers with other family members (Feng *et al.* 2002), it is possible that some mutations are in protein domains that are necessary for dimerization and/or ligand binding. Alternatively, the developmental delay could perturb crucial timed events that may eventually lead to embryonic death.

Each of the *Odz4* alleles fails to complement the *m1* mutation, as well as the $Tyr^{1FDFoHrc}$ deletion (Rinchik and Carpenter 1999). Crosswise pair matings of the *m1*, *m4*, and *m5* alleles result in the compound heterozygotes having the phenotype of the less severe allele, as expected for hypomorphic mutations. However, mutant phenotypes from complementation analyses using the *m3* allele indicate that this allele behaves differently. In matings with *m1* and *m4*, the compound heterozygous mutants have the phenotype of the more severe (*m1* or *m4*), not the less severe, *m3* allele, indicating that this mutation is not a protein hypomorph. Notably, *m3* homozygotes often survive to E11.5, showing neural ectoderm abnormalities that are distinct from the mesodermal anomalies of the other alleles. Importantly, *m3* hemizygotes (*m3*/deletion) have a phenotype that is similar to the *m3* homozygotes (data not shown). However, when the *m3* heterozygotes are mated with *m5*

heterozygotes, the resulting compound heterozygous progeny are viable with a phenotype that is similar to the paternal *m6* defects.

Although intragenic complementation is rarely reported in mammals, the observation of a phenotype, albeit less severe, is expected. It is possible that the *m3* lesion affects a tissue-specific transcript that is also disrupted in the *m1* and *m4* alleles, but not in the *m5* allele. In this scenario, one would assume that the transcriptional levels of *Odz4* are crucial for normal development. Alternatively, since ODZ4 is predicted to produce secreted peptides, and it is probable that the protein is cleaved into multiple protein fragments (Dgany and Wides 2002). It is interesting to speculate that the individual mutations may affect more than one protein product. This may account for some or all of the phenotypic variation that we see among the different mutants and could explain why we see intragenic complementation between the *m3* and *m5* alleles. Another explanation could stem from the necessity of ODZ4 to dimerize with itself and other family members (Feng *et al.* 2002). Although none of the alleles has an obvious heterozygous phenotype, it is possible that the lesion in the *m3* mutation could have deleterious effects in combination with the *m1* and *m4* alleles. The behavior of the *m3* allele indicates that protein interactions are the most likely cause of the interesting genetic interactions between *m3* and the other alleles.

The non-Mendelian pattern of inheritance of the *m6* allele is unique. The lethal phenotype of the maternally inherited *m6* defect initially manifests as developmental delay, but then proceeds to specific abnormalities in older embryos, including kinky neural tubes, incomplete turning, limb abnormalities, and vasculature defects. Since these phenotypes are observed anytime from E8.5 onward, the expression of *Odz4* in the mesoderm (E7.5), neural ectoderm (E8.5), tail bud (E11.5), and limbs (E11.5) is very consistent with these abnormalities. The viable phenotype (paternal *m6* defect) is also consistent with defects in *Odz4*. These animals are often runted at birth and weaning and can have skeletal abnormalities. Since the skeleton is derived from the somites, a subtle defect in somite differentiation could easily give rise to vertebrate fusions and abnormalities.

What could cause this differing pattern of inheritance? The first possibility is that genomic imprinting could account for the differential phenotype. This is an attractive hypothesis, as only maternal inheritance of the *m6* mutation results in a lethal phenotype. However, the genetics involved in the *m6* allele are more complicated, as this phenotype manifests only in a hemizygous form (*i.e.*, *m6*/deletion); the *m6/m6* homozygous animals are viable and have the same phenotype as the paternally inherited *m6* hemizygotes. Another strong possibility is that *Odz4* is a mammalian maternal effect gene. Although common in Drosophila, there are few examples of maternally expressed oocyte-specific genes in mammals (Tong *et al.* 2004). If the *m6* allele lies in a transcript that is laid down in the oocyte during oogenesis, it is possible that the presence of a nonfunctional maternal *m6* allele coupled with one copy of the mutated zygotic allele could explain the phenotypic differences observed in the *m6* mutants.

The finding of a nonconservative amino acid substitution in the *m4* allele of *l7Rn3* indicates that *Odz4* is a very strong candidate for the allele series. We predict that this Ala 2642 Pro substitution, which stems from a G-to-C transversion in the globular domain, would disrupt important protein-protein interactions. We hypothesize that disruption of cellular contacts would cause a delay in mesoderm induction as well as failure of the allantois to migrate and fuse with the chorion. Both of these phenotypes are seen in the *Odz4* mutants. However, we have been unable to find another mutation within the coding region in the other mutants by sequencing RT-PCR products or heterozygous genomic DNA.

To find a mutation by sequencing RT-PCR products, it is crucial to analyze the correct tissue, and this method often fails to identify all mutations (Walkowicz *et al.* 1999). In lethal alleles, we can sequence only template made from RNA derived from whole embryos. If the lesion lies in a rare message, the other normal transcripts could easily mask the mutation. Although not well publicized, it has been shown that detection of a lesion in heterozygous DNA is not always possible (Papathanasiou *et al.* 2003). In this case, a dominant mutation was detected by sequencing homozygous RT-PCR products, but could not be identified by sequencing heterozygous DNA. In heterozygous DNA, it is possible that the wild-type allele amplifies more efficiently, that the incorporation of the BigDye-labeled nucleotide is biased, or that a heterozygous lesion is missed in reading sequence traces. A final possibility is that the mutations in the other alleles are located in unidentified tissue-specific exons or within the noncoding regions that are crucial for directing tissue-specific or temporal expression of *Odz4*. These mutations could reside outside of the critical region within other, as-yet-unidentified *Odz4* transcripts. Since our crossover data have eliminated genes that lie proximal to the translation start site, the possibility that these mutations would be in other genes is unlikely. Although many lesions for ENU-induced allelic series remain elusive, none have been reported in defined regulatory elements to date (Guenet 2004).

Here, we have shown that *Odz4* is involved in determining the anterior-posterior axis in mice. The Drosophila *Odz* (*Ten^{m}*) ortholog displays a pair-rule phenotype, with expression occurring in alternating parasegments. TENM is a transmembrane domain protein that is cleaved into multiple membrane-bound and soluble protein isoforms (Dgany and Wides 2002), each of which may play an important role during development. The other fly ortholog, *Ten^{a}*, is expressed in the CNS, brain, and hindgut during development (Fascetti and Baumgartner 2002).

Phylogenetic analysis indicates that either of these two genes could be the ortholog of *Odz4* (Minet and Chiquet-Ehrismann 2000). In the mouse, *Odz4* has three additional homologs, which are all members of the TENEURIN protein family. TENEURINS, cell-surface signaling molecules that are highly expressed in the developing CNS, may play a role in limb development, somite formation, and the patterning of neural connections (Rubin *et al.* 1999; Tucker *et al.* 2001). Although no proteins outside of ODZ family members share significant homology distal to the transmembrane region, the EGF repeats and transmembrane domain located within the N terminus share significant homology with several members of the NOTCH pathway, including NOTCH, SERATE, CRUMBS, and DELTA (Ben-Zur *et al.* 2000; Dgany and Wides 2002). NOTCH signaling is necessary for development of the pancreas (an endoderm-derived organ) and neuronal lineages (ectoderm-derived tissues), as well as hematopoietic cells, the skeleton, and vasculature (mesoderm-derived tissues; reviewed in Harper *et al.* 2003). Further, NOTCH signaling plays a major role in somite segmentation (reviewed in Rida *et al.* 2004), a process that is clearly disrupted in our mutants. Therefore, it is tempting to speculate that we have discovered a new member of the extended NOTCH signaling cascade.

The authors thank Temenit Asgedom for excellent technical support and Alec Wang for kindly supplying the 3.2.5 and 6.11 *Odz4* cDNAs. We also thank Sally Camper, Richard Behringer, Tom Meehan, and Kathy Hentges for critically evaluating this manuscript. This work was supported by National Institutes of Health (NIH) fellowship 1F32HD44407 to A.C.L., a Kleberg Foundation grant to M.J.J., and an NIH grant U01HD39372 to M.J.J.

LITERATURE CITED

Adelaide, J., M. Chaffanet, M. J. Mozziconacci, C. Popovici, N. Conte *et al.*, 2000 Translocation and coamplification of loci from chromosome arms 8p and 11q in the MDA-MB-175 mammary carcinoma cell line. Int. J. Oncol. **16:** 683–688.

Alessandrini, F., T. Jakob, A. Wolf, E. Wolf, R. Balling *et al.*, 2001 Enu mouse mutagenesis: generation of mouse mutants with aberrant plasma IgE levels. Int. Arch. Allergy Immunol. **124:** 25–28.

Baumgartner, S., and R. Chiquet-Ehrismann, 1993 Tena, a Drosophila gene related to tenascin, shows selective transcript localization. Mech. Dev. **40:** 165–176.

Baumgartner, S., D. Martin, C. Hagios and R. Chiquet-Ehrismann, 1994 Tenm, a Drosophila gene related to tenascin, is a new pair-rule gene. EMBO J. **13:** 3728–3740.

Ben-Zur, T., E. Feige, B. Motro and R. Wides, 2000 The mammalian Odz gene family: homologs of a Drosophila pair-rule gene with expression implying distinct yet overlapping developmental roles. Dev. Biol. **217:** 107–120.

Boue, S., I. Letunic and P. Bork, 2003 Alternative splicing and evolution. BioEssays **25:** 1031–1034.

Church, G., and W. Gilbert, 1984 Genomic sequencing. Proc. Natl. Acad. Sci. USA **81:** 1991–1995.

Dgany, O., and R. Wides, 2002 The Drosophila odz/ten-m gene encodes a type I, multiply cleaved heterodimeric transmembrane protein. Biochem. J. **363:** 633–643.

Echelard, Y., D. J. Epstein, B. St-Jacques, L. Shen, J. Mohler *et al.*, 1993 Sonic hedgehog, a member of a family of putative signaling molecules, is implicated in the regulation of CNS polarity. Cell **75:** 1417–1430.

Fascetti, N., and S. Baumgartner, 2002 Expression of Drosophila Ten-a, a dimeric receptor during embryonic development. Mech. Dev. **114:** 197–200.

Fedorova, L., and A. Fedorov, 2003 Introns in gene evolution. Genetica **118:** 123–131.

Feng, K., X. H. Zhou, T. Oohashi, M. Morgelin, A. Lustig *et al.*, 2002 All four members of the Ten-m/Odz family of transmembrane proteins form dimers. J. Biol. Chem. **277:** 26128–26135.

Gibson, F., J. Walsh, P. Mburu, A. Varela, K. A. Brown *et al.*, 1995 A type VII myosin encoded by the mouse deafness gene *shaker-1*. Nature **374:** 62–64.

Graw, J., J. Loster, D. Soewarto, H. Fuchs, A. Reis *et al.*, 2002 V76D mutation in a conserved gD-crystallin region leads to dominant cataracts in mice. Mamm. Genome **13:** 452–455.

Guenet, J.-L., 2004 Chemical mutagenesis of the mouse genome: an overview, pp. 9–24 in *Genetica: Mutagenesis of the Mouse Genome*, edited by M. J. Justice and M. A. Bedell. Kluwer Academic, Dordrecht, The Netherlands.

Hardison, R. C., 2003 Comparative genomics. PLoS Biol. **1:** E58.

Hardisty, R. E., P. Mburu and S. D. Brown, 1999 ENU mutagenesis and the search for deafness genes. Br. J. Audiol. **33:** 279–283.

Harper, J. A., J. S. Yuan, J. B. Tan, I. Visan and C. J. Guidos, 2003 Notch signaling in development and disease. Clin. Genet. **64:** 461–472.

Hrabe de Angelis, M., and H. Flaswinkel, 2000 Genome wide large scale production of mutant mice by ENU mutagenesis. Nat. Genet. **25:** 444–447.

Isaacs, A. M., K. E. Davies, A. J. Hunter, P. M. Nolan, L. Vizor *et al.*, 2000 Identification of two new Pmp22 mouse mutants using large-scale mutagenesis and a novel rapid mapping strategy. Hum. Mol. Genet. **9:** 1865–1871.

Karolchik, D., R. Baertsch, M. Diekhans, T. S. Furey, A. Hinrichs *et al.*, 2003 The UCSC Genome Browser Database. Nucleic Acids Res. **31:** 51–54.

Kerlavage, A., V. Bonazzi, M. di Tommaso, C. Lawrence, P. Li *et al.*, 2002 The Celera Discovery System. Nucleic Acids Res. **30:** 129–136.

Kile, B. T., K. E. Hentges, A. T. Clark, H. Nakamura, A. P. Salinger *et al.*, 2003 Functional genetic analysis of mouse chromosome 11. Nature **425:** 81–86.

Lee, C. J., and K. Irizarry, 2003 Alternative splicing in the nervous system: an emerging source of diversity and regulation. Biol. Psychiatry **54:** 771–776.

Levine, A., A. Bashan-Ahrend, O. Budai-Hadrian, D. Gartenberg, S. Menasherow *et al.*, 1994 Odd Oz: a novel Drosophila pair rule gene. Cell **77:** 587–598.

Liu, X., E. Baker, H. J. Eyre, G. R. Sutherland and M. Zhou, 1999 Gamma-heregulin: a fusion gene of DOC-4 and neuregulin-1 derived from a chromosome translocation. Oncogene **18:** 7110–7114.

Lossie, A. C., M. S. Buckwalter and S. A. Camper, 1993 Lysyl oxidase (Lox) maps between Grl-1 and Adrb-2 on mouse chromosome 18. Mamm. Genome **4:** 177–178.

Minet, A. D., and R. Chiquet-Ehrismann, 2000 Phylogenetic analysis of teneurin genes and comparison to the rearrangement hot spot elements of E. coli. Gene **257:** 87–97.

Nagy, A., M. Gertenstein, K. Vintersten and R. R. Behringer, 2003 *Manipulating the Mouse Embryo: A Laboratory Manual*. Cold Spring Harbor Laboratory Press, Cold Spring Harbor, NY.

Nolan, P. M., D. Kapfhamer and M. Bucan, 1997 Random mutagenesis screen for dominant behavioral mutations in mice. Methods **13:** 379–395.

Nolan, P. M., J. Peters, M. Strivens, D. Rogers, J. Hagan *et al.*, 2000 A systematic, genome-wide, phenotype-driven mutagenesis programme for gene function studies in the mouse. Nat. Genet. **25:** 440–443.

Oohashi, T., X. H. Zhou, K. Feng, B. Richter, M. Morgelin *et al.*, 1999 Mouse ten-m/Odz is a new family of dimeric type II transmembrane proteins expressed in many tissues. J. Cell Biol. **145:** 563–577.

Papathanasiou, P., A. C. Perkins, B. S. Cobb, R. Ferrini, R. Sridharan *et al.*, 2003 Widespread failure of hematolymphoid differentiation caused by a recessive niche-filling allele of the Ikaros transcription factor. Immunity **19:** 131–144.

Rida, P. C., N. Le Minh and Y. J. Jiang, 2004 A Notch feeling of somite segmentation and beyond. Dev. Biol. **265:** 2–22.

Rinchik, E. M., and D. A. Carpenter, 1993 N-ethyl-N-nitrosourea-

induced prenatally lethal mutations define at least two complementation groups within the embryonic ectoderm development (eed) locus in mouse chromosome 7. Mamm. Genome **4:** 349–353.

Rinchik, E. M., and D. A. Carpenter, 1999 *N*-ethyl-*N*-nitrosourea mutagenesis of a 6- to 11-cM subregion of the Fah-Hbb interval of mouse chromosome 7: completed testing of 4557 gametes and deletion mapping and complementation analysis of 31 mutations. Genetics **152:** 373–383.

Rinchik, E. M., D. A. Carpenter and P. B. Selby, 1990 A strategy for fine-structure functional analysis of a 6- to 11-centimorgan region of mouse chromosome 7 by high-efficiency mutagenesis. Proc. Natl. Acad. Sci. USA **87:** 896–900.

Rubin, B. P., R. P. Tucker, D. Martin and R. Chiquet-Ehrismann, 1999 Teneurins: a novel family of neuronal cell surface proteins in vertebrates, homologous to the Drosophila pair-rule gene product Ten-m. Dev. Biol. **216:** 195–209.

Russell, L. B., 1989 Functional and structural analyses of mouse genomic regions screened by the morphological specific-locus test. Mutat. Res. **212:** 23–32.

Russell, W. L., and L. B. Russell, 1959 The genetic and phenotypic characteristics of radiation-induced mutations in mice. Radiat. Res. **1** (Suppl.): 296–305.

Soewarto, D., C. Fella, A. Teubner, B. Rathkolb, W. Pargent *et al.*, 2000 The large-scale Munich ENU-mouse-mutagenesis screen. Mamm. Genome **11:** 507–510.

Tong, Z. B., L. Gold, A. De Pol, K. Vanevski, H. Dorward *et al.*, 2004 Developmental expression and subcellular localization of mouse MATER, an oocyte-specific protein essential for early development. Endocrinology **145:** 1427–1434.

Tucker, R. P., R. Chiquet-Ehrismann, M. P. Chevron, D. Martin, R. J. Hall *et al.*, 2001 Teneurin-2 is expressed in tissues that regulate limb and somite pattern formation and is induced in vitro and in situ by FGF8. Dev. Dyn. **220:** 27–39.

Vivian, J. L., Y. Chen, D. Yee, E. Schneider and T. Magnuson, 2002 An allelic series of mutations in Smad2 and Smad4 identified in a genotype-based screen of N-ethyl-N- nitrosourea-mutagenized mouse embryonic stem cells. Proc. Natl. Acad. Sci. USA **99:** 15542–15547.

Walkowicz, M., Y. Ji, X. Ren, B. Horsthemke, L. B. Russell *et al.*, 1999 Molecular characterization of radiation- and chemically induced mutations associated with neuromuscular tremors, runting, juvenile lethality, and sperm defects in jdf2 mice. Mamm. Genome **10:** 870–878.

Wang, X. Z., M. Kuroda, J. Sok, N. Batchvarova, R. Kimmel *et al.*, 1998 Identification of novel stress-induced genes downstream of chop. EMBO J. **17:** 3619–3630.

Waterston, R. H., K. Lindblad-Toh, E. Birney, J. Rogers, J. F. Abril *et al.*, 2002 Initial sequencing and comparative analysis of the mouse genome. Nature **420:** 520–562.

Zdobnov, E. M., and R. Apweiler, 2001 InterProScan—an integration platform for the signature-recognition methods in InterPro. Bioinformatics **17:** 847–848.

Zhao, S., and C. W. Hill, 1995 Reshuffling of Rhs components to create a new element. J. Bacteriol. **177:** 1393–1398.

Zhou, X. H., O. Brandau, K. Feng, T. Oohashi, Y. Ninomiya *et al.*, 2003 The murine Ten-m/Odz genes show distinct but overlapping expression patterns during development and in adult brain. Gene Expr. Patterns **3:** 397–405.

Communicating editor: N. A. Jenkins